Journal of Biomolecular NMR, 8 (1996) 345–350
ESCOM

J-Bio NMR 398

Phase labeling of C-H and C-C spin-system topologies: Application in constant-time PFG-CBCA(CO)NH experiments for discriminating amino acid spin-system types

Carlos B. Rios, Wenqing Feng, Mitsuru Tashiro, Zhigang Shang and Gaetano T. Montelione*

Center for Advanced Biotechnology and Medicine and Department of Molecular Biology and Biochemistry, Rutgers University, Piscataway, NJ 08854-5638, U.S.A.

Received 12 July 1996
Accepted 30 September 1996

Keywords: Automated analysis of NMR data; Protein NMR; Pulsed-field gradient; Resonance assignments; Triple resonance

Summary

Triple-resonance experiments facilitate the determination of sequence-specific resonance assignments of medium-sized $^{13}C,^{15}N$-enriched proteins. Some triple-resonance experiments can also be used to obtain information about amino acid spin-system topologies by proper delay tuning. The constant-time PFG-CBCA(CO)NH experiment allows discrimination between five different groups of amino acids by tuning (phase labeling) independently the delays for proton–carbon refocusing and carbon–carbon constant-time frequency labeling. The proton–carbon refocusing delay allows discrimination of spin-system topologies based on the number of protons attached to C^{α} and C^{β} atoms (i.e. C-H phase labeling). In addition, tuning of the carbon–carbon constant-time frequency-labeling delay discriminates topologies based on the number of carbons directly coupled to C^{α} and C^{β} atoms (i.e. C-C phase labeling). Classifying the spin systems into these five groups facilitates identification of amino acid types, making both manual and automated analysis of assignments easier. The use of this pair of optimally tuned PFG-CBCA(CO)NH experiments for distinguishing five spin-system topologies is demonstrated for the 124-residue bovine pancreatic ribonuclease A protein.

Sequence-specific resonance assignments provide the basis for interpretation of multidimensional NMR spectra and determination of 3D structures of macromolecules (Wüthrich, 1986; Clore and Gronenborn, 1991), and triple-resonance experiments (Montelione and Wagner, 1989,1990; Ikura et al., 1990; Bax and Grzesiek, 1993) provide an important approach for determining these assignments in proteins. Recent efforts in developing automated approaches for analysis of triple-resonance data (reviewed by Zimmerman and Montelione (1995)) have focused on obtaining information that is useful for classifying amino acid spin-system types (Montelione et al., 1992; Grzesiek et al., 1993; Lyons and Montelione, 1993; Wittekind et al., 1993; Yamazaki et al., 1993,1995; Olejniczak and Fesik, 1994; Gehring and Guittet, 1995; Tashiro et al., 1995; Dötsch and Wagner, 1996; Dötsch et al., 1996a,b; Farmer and Venters, 1996; Feng et al., 1996). This information is extremely valuable for determining resonance assignments, especially when combined with characteristic ^{13}C chemical shift data in automated assignment programs (Friedrichs et al., 1994; Meadows et al., 1994; Zimmerman et al., 1994; Zimmerman and Montelione, 1995).

Information about spin-system topologies can be obtained by appropriate tuning of scalar coupling effects. For example, constant-time frequency-evolution periods commonly used in triple-resonance experiments are generally designed to combine frequency evolution and coherence defocusing/refocusing periods (Powers et al., 1991; Clubb and Wagner, 1992; Kay et al., 1992a; Olejniczak et al., 1992; Palmer et al., 1992). During these coherence defocusing/refocusing periods, magnetization oscillates differently depending on the spin-system topology and the set of active and passive scalar couplings. In uniformly ^{13}C-enriched molecules, proper tuning of these delay times can provide ^{13}C resonance 'phase' information (i.e., positive or negative peak intensities) that depends on the number of coupled ^{13}C nuclei (Grzesiek and Bax,

*To whom correspondence should be addressed.

1992a,1993; Santoro and King, 1992; Tashiro et al., 1995; Feng et al., 1996). We refer to these as 'C-C-type phase experiments'. Alternatively, proper tuning of the time period used for refocusing (or defocusing) antiphase $H_zC_{x,y}$ carbon magnetization into (or from) in-phase carbon magnetization can provide ^{13}C resonance phase information that depends on the number of coupled ^1H nuclei (Grzesiek and Bax, 1993; Tashiro et al., 1995; Feng et al., 1996). We refer to these as 'C-H-type phase experiments'. Such 'phase experiments' can be used to identify spin-system topologies that are characteristic of different amino acid residue types (see for example Grzesiek and Bax (1993) and Tashiro et al. (1995)) and thus restrict the spin system to a subset of possible amino acid residue types.

In our efforts to develop automated methods for determining resonance assignments in proteins, we have found that it is convenient to incorporate 'phase labeling' directly into the standard experiments used for establishing intraresidue and/or sequential ($C_i^\beta / C_i^\alpha / H_i^\alpha \rightarrow NH_i$ or $C_i^\beta / C_i^\alpha / H_i^\alpha \rightarrow NH_{i+1}$) connectivities. For example, in a recent publication (Feng et al., 1996) we have compared 'C-C phase' and 'C-H phase' versions of 3D constant-time (CT) pulsed-field gradient (PFG) HACANH and HACA(CO)NH experiments for distinguishing glycine from non-glycine spin systems and observed that in some cases the 'phase' versions of the CT-HACANH experiment can exhibit signal-to-noise ratios higher than those of non-phase data run with identical total collection times. C-C phase labeling has also been used in the HCC(CO)NH-TOCSY experiment to discriminate spin-system topologies based on the numbers of ^{13}C atoms attached to each side-chain carbon (Tashiro et al., 1995); Grzesiek and Bax have used C-C phase information in the CBCANH experiment to differentiate between non-glycine C^α and C^β nuclei (Grzesiek and Bax, 1992a) and to identify C^β resonances coupled to aromatic or carbonyl carbons (Grzesiek and Bax, 1993). More recently, an optimally tuned and appropriately phase-cycled PFG-CBCA(CO)NH ex-

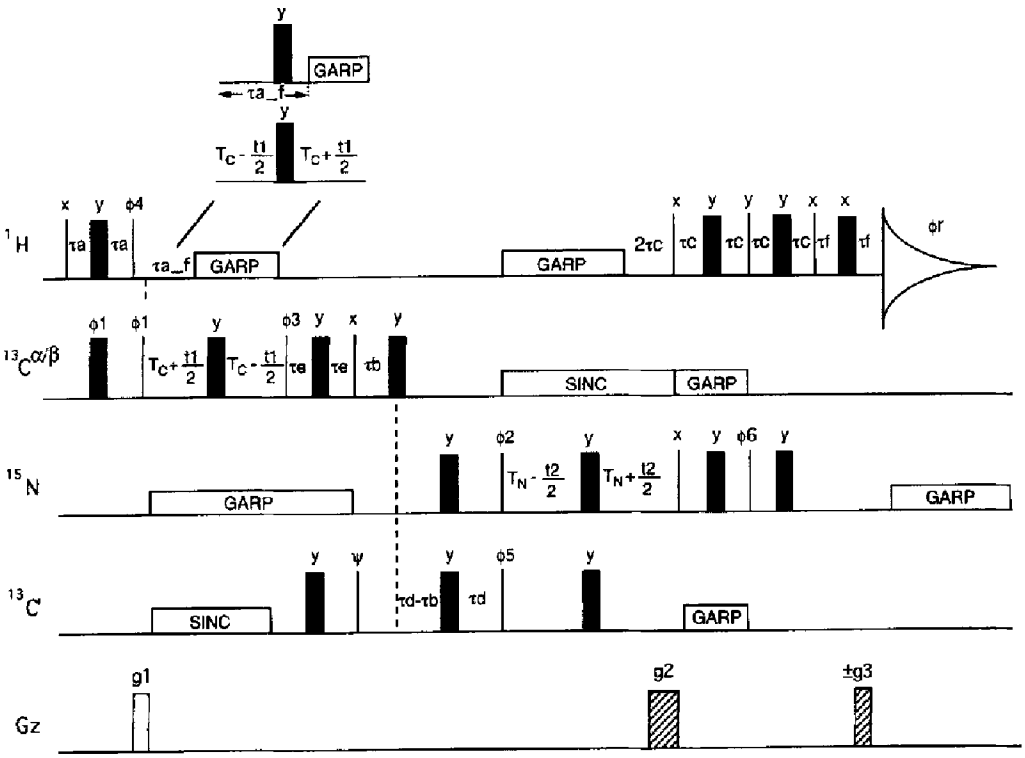

Fig. 1. Pulse sequence for 3D CT PFG-CBCA(CO)NH. The narrow and thick vertical lines represent 90° and 180° pulses, respectively. The insert shows the variant implemented by the pulse sequence program for τ_{a_f} values greater than T_C. The pulses are phase cycled as follows: $\phi1 = +x,-x$, $\phi2 = 8(+x),8(-x)$, $\phi3 = +x,-x,-x,+x,-x,+x,+x,-x,-x,+x,+x,-x,+x,-x,-x,+x$, $\phi4 = 4(+y),4(-y)$, $\phi5 = 2(+x),2(-x)$, $\psi = +x$ plus small angle phase shifts to compensate for phase errors introduced by off-resonance decoupling (McCoy and Mueller, 1992; Vuister and Bax, 1992), and the receiver phase $\phi r = +,-,-,+,-,+,+,-,-,+,+,-,+,-,-,+$. The phase cycle $\phi2$ is optional. Pulsed-field gradients (G_z) are applied along the z-axis. Gradient g1 is a heteronuclear zz-filter, while gradients g2 and g3 are used for coherence pathway selection. The proton carrier is set at ~2.5 ppm until the $^{13}C' \rightarrow {}^{15}N$ coherence transfer, at which point it is reset to the center of the H^N region, and the aliphatic ^{13}C carrier frequency is set at about 35 ppm until the $^{15}N \rightarrow H^N$ coherence transfer, at which point it is reset to a frequency midway between the $^{13}C'$ and $^{13}C^\alpha$ regions. Wide-band GARP (Shaka et al., 1985) and band-selective sinc (SINC) decoupling schemes are executed from waveform generators. Quadrature detection in the t_1 dimension is obtained by changing the phase $\phi1$ in the States–TPPI manner (Marion et al., 1989). For quadrature detection in the t_2 dimension, N-type and P-type spectra are collected by inverting the phases of $\phi6$ and g3 simultaneously, and combined to give pure phase spectra with sensitivity enhancement (Kay et al., 1992b). These pulse sequences and decoupling waveforms were executed on a three-channel Varian Unity 500 NMR spectrometer, equipped with a fourth synthesizer for C' decoupling, and are available by anonymous ftp from nmrlab.cabm.rutgers.edu or over the world-wide web at http://www-nmr.cabm.rutgers.edu/.

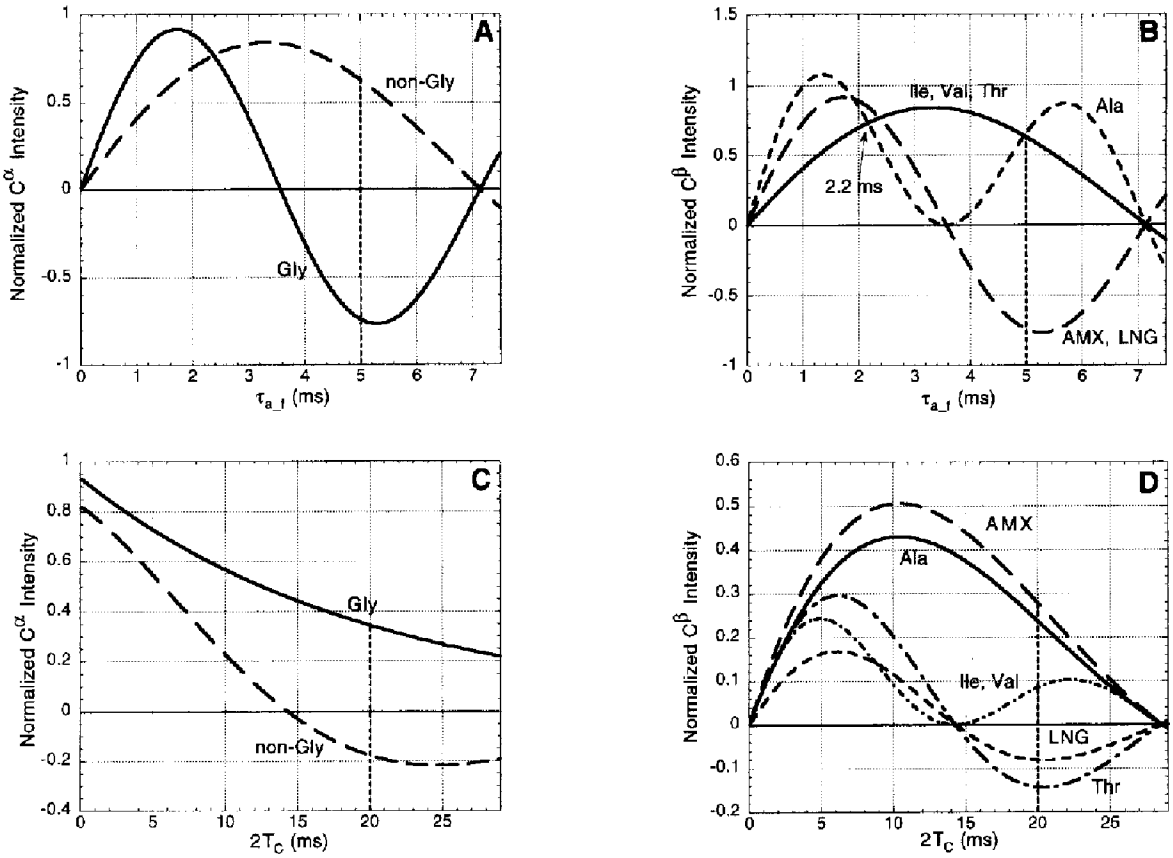

Fig. 2. The dependence of magnetization transfer functions for C^{α} and C^{β} intensities with respect to (A,B) τ_{a_f} and (C, D) $2T_C$ in the PFG-CBCA(CO)NH experiment of Fig. 1. Curves were generated from Eqs. 1, 2 and 3 with $^1J(C^{\alpha}\text{-}H^{\alpha}) = 128$ Hz, $^1J(C^{\beta}\text{-}H^{\beta}) = 128$ Hz, $^1J(C^{\alpha}\text{-}C^{\beta}) = 35$ Hz, $^1J(C^{\beta}\text{-}C^{\gamma}) = 35$ Hz, and a uniform $T_{2,eff} = 20$ ms.

periment has been described to select spin systems with β-methine carbons (i.e. Thr, Val and Ile) (Dötsch et al., 1996a) by tuning the C-H refocusing delay to provide a null intensity for spin systems with β-methylene carbons. PFG-CBCA(CO)NH experiments have also been described for selecting spin systems with (or without) $^{13}C^{\beta}$-$^{13}C^{\gamma}$ couplings (Dötsch and Wagner, 1996; Dötsch et al., 1996b) by tuning the constant-time period to suppress $^{13}C^{\beta}$ nuclei that are not coupled (or coupled) to C^{γ} nuclei.

The use of cross-peak phase information for spin-system identification may be more reliable than schemes that provide suppression of specific spin-system topologies (Gehring and Guittet, 1995; Dötsch et al., 1996a,b), as peaks may not be observed in these spectra for reasons other than the topology filter, and because the desired suppression may not be complete for the filtered resonances. In this communication, we describe a pair of optimally tuned CT PFG-CBCA(CO)NH experiments (Grzesiek and Bax, 1992b,1993; Muhandiram and Kay, 1994), providing phase information on C^{α} and C^{β} cross peaks that depends on the number of directly coupled ^{13}C and ^1H nuclei. The *combination* of C-C and C-H phase information allows distinction between five types of amino acid spin systems: Gly, Ala/Ile/Val, AMX-type, long (LNG)-type, and Thr. This pair of experiments provides data for establishing sequential connections between backbone ^1H, $^{13}C^{\alpha}$, $^{13}C^{\beta}$, and ^{15}N atoms with good sensitivity, while simultaneously yielding phase information on C^{β} atoms that can be used to characterize the corresponding amino acid spin systems.

In the CT PFG-CBCA(CO)NH experiment (Fig. 1), the magnetization starts on H^{α} and H^{β} nuclei. It is then transferred to C^{α} and C^{β}, respectively, by an INEPT transfer (Morris and Freeman, 1979), followed by the refocusing of C^{α} and C^{β} magnetization with respect to their corresponding attached protons during the τ_{a_f} period. During the remaining portion of the CT period $2T_C$, the C^{β} magnetization is frequency labeled and evolves into antiphase with respect to C^{α}. In addition, the C^{α} magnetization that started on the H^{α} nucleus is also frequency labeled. At the end of the $2T_C$ period, the magnetization of interest is given by:

$$-2C_x^{\alpha}\sin(\pi J_{C^{\alpha}H^{\alpha}}\tau_{a\_f})\cos(\pi J_{C^{\alpha}H^{\alpha}}\tau_{a\_f})\cos(\omega_{C^{\alpha}}t_1) \times \exp(-2T_C/T_{2,eff}) \quad (1)$$

and

$$-C_x^{\alpha}\sin(\pi J_{C^{\alpha}H^{\alpha}}\tau_{a\_f})\cos(\pi J_{C^{\alpha}C^{\beta}}2T_C)\cos(\omega_{C^{\alpha}}t_1) \times \exp(-2T_C/T_{2,eff}) \quad (2)$$

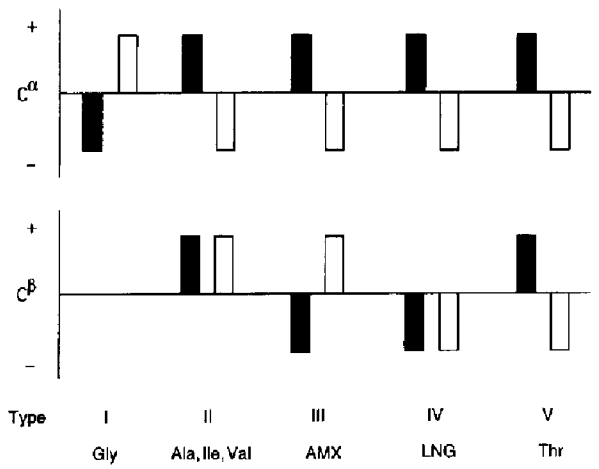

Fig. 3. Diagram of the phase patterns for aliphatic carbon resonances of five different amino acid spin-system types obtained using the pulse sequence in Fig. 1. Solid and open bars represent the data obtained using the C-H and C-C versions, respectively, of the CT PFG-CBCA(CO)NH experiment. Positive and negative resonance phases are represented as up and down bars, respectively.

for magnetization originating from the glycine and non-glycine H^{α}, respectively, and

$$-n2C_y^{\beta}C_z^{\alpha}\sin(\pi J_{C^{\beta}H^{\beta}}\tau_{a\_f})\cos^{n-1}(\pi J_{C^{\beta}H^{\beta}}\tau_{a\_f}) \times \cos^{q}(\pi J_{C^{\beta}C^{\gamma}}2T_C)\sin(\pi J_{C^{\alpha}C^{\beta}}2T_C) \times \cos(\omega_{C^{\beta}}t_1)\exp(-2T_C/T_{2,eff}) \quad (3)$$

for magnetization originating from H^{β}, where τ_{a_f} and $2T_C$ are the proton refocusing and carbon–carbon constant-time periods, respectively, $J_{C^{\alpha}H^{\alpha}}$, $J_{C^{\beta}H^{\beta}}$, $J_{C^{\alpha}C^{\beta}}$, and $J_{C^{\beta}C^{\gamma}}$ are the one-bond $^1J(C^{\alpha}\text{-}H^{\alpha})$, $^1J(C^{\beta}\text{-}H^{\beta})$, $^1J(C^{\alpha}\text{-}C^{\beta})$, and $^1J(C^{\beta}\text{-}C')$ coupling constants, respectively, ω_C's are carbon resonance frequencies, n and q are the number of proton and carbon atoms directly coupled to C^{β} atoms, respectively, and $T_{2,eff}$ is an effective relaxation time for coherences during the $2T_C$ period. Although the magnetization actually passes through different coherence states and may exhibit multi-exponential relaxation, we make the simplifying assumption that during the entire $2T_C$ period the coherences on the pathway of interest relax with a single, effective relaxation time $T_{2,eff}$.

Appropriate selection of the delays τ_{a_f} and $2T_C$ allows phase labeling of the C^{α} and C^{β} carbon resonances during the t_1 frequency-evolution period, which depends on the proton and carbon multiplicities of the C^{α} or C^{β} atoms. Figures 2A and B show the dependence of these transfer functions with respect to the C-H phase-labeling delay τ_{a_f}, with $T_{2,eff} = 20$ ms. There is an optimal value for positive intensity at ~2.2 ms for all proton multiplicities and another optimal value at ~5 ms, which gives negative intensities for all methylene C^{α} (i.e. Gly) and C^{β} resonances. Values τ_{a_f} of ~5 ms will thus 'phase discriminate' between spin systems with odd and even numbers of protons directly coupled to C^{α} or C^{β} atoms. Computer simulations of this transfer function, carried out with uniform effective relaxation times $T_{2,eff}$ ranging from 5 to 50 ms, indicate that the optimal value for this C-H phase discrimination remains constant at $\tau_{a\_f} \approx 5.0$ ms.

Figures 2C and D show the dependence of these transfer functions with respect to the C-C phase-labeling delay $2T_C$, assuming τ_{a_f} is set to its 'non-phase' optimum of 2.2 ms and with $T_{2,eff} = 20$ ms. Optimal values occur at 4–8 ms, resulting in positive intensities for all C^{β} and C^{α} carbon multiplicities, and at ~18–20 ms, providing positive intensities for C^{α} resonances of Gly and C^{β} resonances of Ala, Ile, Val, Asp, Asn, Cys, His, Phe, Ser, Tyr, and Trp spin systems, and negative intensities for C^{α} resonances of non-Gly and C^{β} resonances of Arg, Gln, Glu, Leu, Lys, Met, Pro, and Thr spin systems. Computer simulations of this transfer function, carried out with effective relaxation times $T_{2,eff}$ ranging from 5 to 50 ms, indicate that the optimal value for this C-C phase discrimination ranges from $2T_C = 17$ to 21 ms, while the amplitudes of the signal at these optima (relative to a normalized amplitude of 1.0 for $T_{2,eff} = \infty$) vary from 0.02 to 0.70.

Using a combination of C-H and C-C phase experiments, one can thus classify amino acid spin systems into five different groups (Fig. 3). The first group (type I) consists of the Gly spin system, which gives negative and positive phases for C^{α} resonances in C-H and C-C experiments, respectively. When the spectra are phased with this convention, all other amino acid spin systems have positive and negative phases, respectively, for C^{α} resonances in the C-H and C-C experiments. The second group (type II) includes the spin systems of Ala, Ile and Val, which have positive phases for C^{β} resonances in both the C-H and C-C versions of the experiment. Although Ile and Val have a significantly different transfer function compared to Ala (Fig. 2), the three spin systems behave similarly at the τ_{a_f} and $2T_C$ values used to discriminate between the other spin-system types. The third group (type III) includes the AMX-type spin systems (i.e., Asn, Asp, Cys, His, Phe, Ser, Tyr and Trp). These have negative phases for C^{β} resonances in the C-H version of the experiment, and positive phases for C^{β} resonances in the C-C version. The fourth group (type IV) comprises the 'LNG-type' amino acid residues (i.e., Arg, Gln, Glu, Leu, Lys, Met and Pro), which have negative phases for C^{β} resonances in both the C-H and C-C versions of the experiment. The fifth group (type V) consists of the Thr spin system, with positive C^{β} phase in the C-H version and negative phases for C^{β} resonances in the C-C version of the CT CBCA-(CO)NH experiment. This phase information aids in the classification of amino acid type and facilitates the determination of sequence-specific assignments by manual or automated analysis (Zimmerman et al., 1994; Zimmerman and Montelione, 1995).

The long $2T_C$ values required for C-C phase labeling can cause a significant reduction in sensitivity. This is

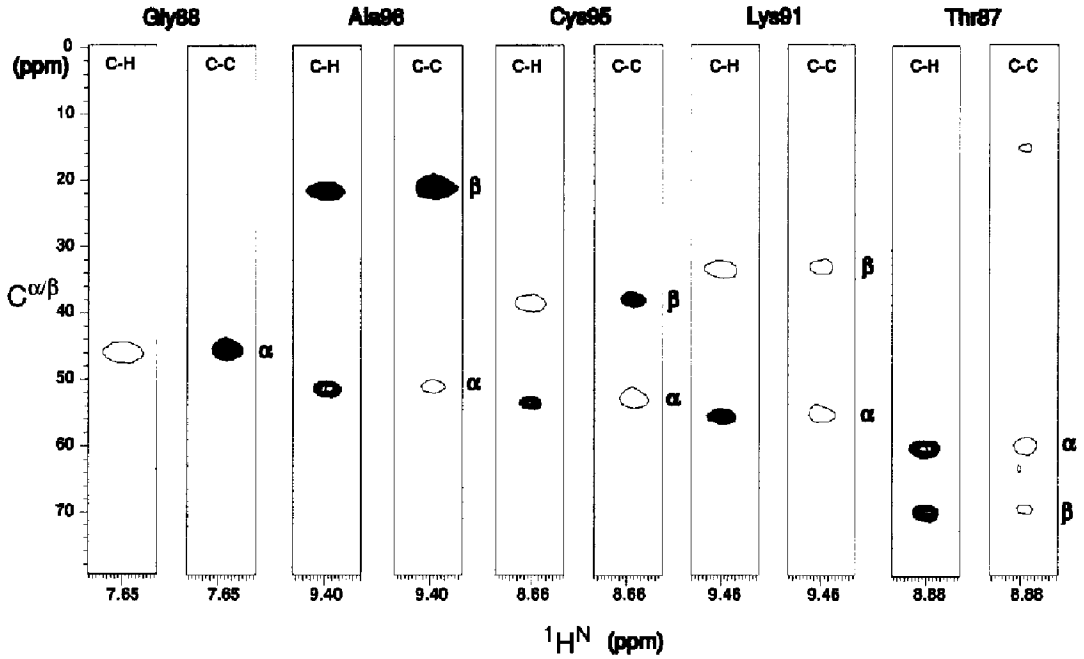

Fig. 4. Representative strip plots from ^{13}C-H^N planes of a 3D CT PFG-CBCA(CO)NH spectrum obtained for RNaseA. Each pair of plots presents data from the C-H and C-C versions, respectively, of the experiment. The width in the H^N dimension of each strip is 0.20 ppm. Additional experimental details are described in the legend of Fig. 5.

especially problematic in larger proteins, in which small $T_{2,eff}$ values greatly attenuate the signal at the $2T_C$ value used for phase labeling. In such larger systems, this same approach can be used for C-C phase labeling in ^2H,^{13}C, ^{15}N-enriched proteins, which have longer ^{13}C $T_{2,eff}$ relaxation times. On the other hand, the longer τ_{a_f} value required for C-H phase labeling does not increase the total experiment time, nor does it decrease the signal-to-noise ratio significantly. Considering that the phase experiments generally exhibit lower signal-to-noise ratios and possible cancellations of cross peaks due to resonance overlap, however, it is prudent to carry them out only as supplements to the higher-sensitivity non-phase PFG-CBCA-(CO)NH experiment.

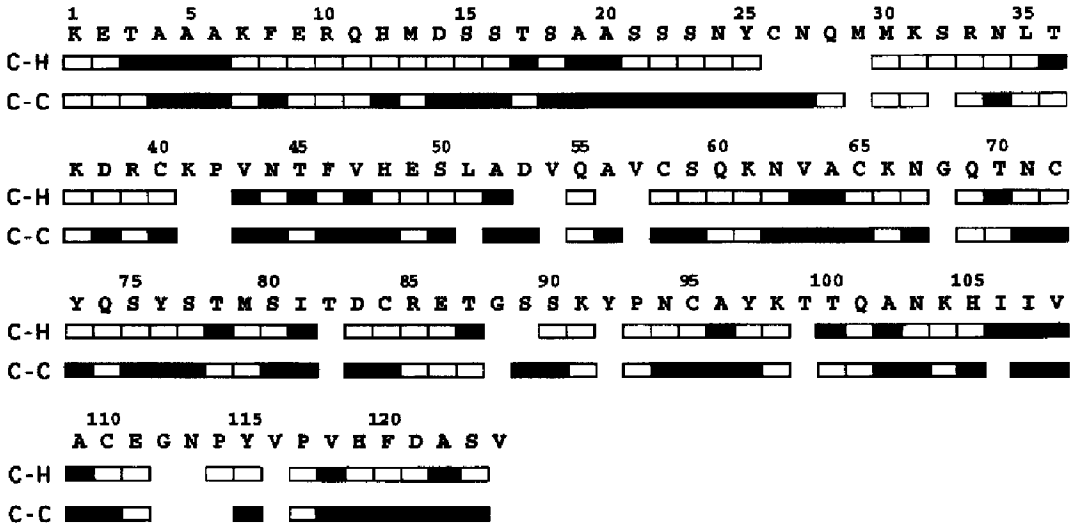

Fig. 5. Summary of 3D CT PFG-CBCA(CO)NH data for C^β resonances recorded with C-H (τ_{a_f} = 5 ms, $2T_C$ = 6 ms) and C-C (τ_{a_f} = 2.2 ms, $2T_C$ = 20 ms) phase labeling. Open and filled boxes indicate positive and negative cross peaks, respectively, in these processed spectra. Data were recorded with the T_N, τ_a, τ_b, τ_c, τ_d, and τ_e delays optimized to 14, 1.3, 4.4, 2.4, 14 and 4.1 ms, respectively, and 16 transients per FID. For both spectra, pulsed-field gradients (G_z) were applied with an amplitude of ≈ 26 G/cm and lengths g1 = 100 μs, g2 = 5.075 ms, and g3 = 500 μs. The delay τ_f = g3 + 150 μs for gradient recovery. The data were collected as 40 * 40 * 512 complex points and zero-filled to 256 * 128 * 2048 points using spectral widths of 10 000, 2500 and 6900 Hz in the ω_1, ω_2 and ω_3 dimensions, respectively. The total collection time for each of these two 3D data sets was about 24 h on a 500 MHz NMR spectrometer. Missing data are attributed in part to overlap between positive and negative cross peaks in the specta, and in part to shorter $T_{2,eff}$ values in some parts of the protein structure.

The C-H and C-C versions of the 3D CT PFG-CBCA-(CO)NH experiment were collected for an engineered 71-residue IgG-binding domain of staphylococcal protein A (Z-domain) and for the 124-residue bovine pancreatic ribonuclease A (RNase A) protein. Figure 4 shows representative strip plots from C-H and C-C CT PFG-CBCA-(CO)NH experiments obtained for the sample of RNase A at 2.0 mM protein concentration. Similar results were obtained for Z-domain. All resolved resonances exhibit the phases expected from the transfer functions shown in Fig. 2. Summaries of the C-H and C-C PFG-CBCA(CO)-NH phase information obtained for RNase A are presented in Fig. 5. Similar 3D experiments have also been carried out using aliphatic proton (instead of carbon) frequency labeling in the ω_1 dimension.

These 'phase experiments' provide useful information for characterizing spin-system types. One can further distinguish amino acid spin systems by combining these phase data with C^{α} and C^{β} chemical shift discriminators (Grzesiek and Bax, 1993; Zimmerman and Montelione, 1995). For example, Ala spin systems are distinguished reliably from the other type II spin systems (Val and Ile) by their characteristic upfield C^{β} frequency range (Wishart et al., 1995). Similarly, Ser spin systems are easily distinguished from the other type III (AMX) spin systems by their characteristic downfield C^{β} frequency range (Wishart et al., 1995). In this way, the combined analysis of data from C-H and C-C phase versions of the CT PFG-CBCA(CO)NH experiment allows discrimination of the following seven amino acid spin-system types: Ala, Gly, Ser, Thr, Val/Ile, AMX (excluding Ser), and LNG-type spin systems. Statistical analysis of the further discriminating power of combined analysis of ^{13}C chemical shift data and C-H / C-C phase information for uniquely identifying other spin-system types is in progress in our laboratory.

Acknowledgements

We thank Dr. D. Zimmerman for helpful discussions, and Ms. R. Watson for editorial comments on the manuscript. This work was supported by grants from The National Institutes of Health (GM-47014, GM-50733), the National Science Foundation (MCB-9407569), a National Science Foundation Young Investigator Award (MCB-9357526), and a Camille Dreyfus Teacher-Scholar Award.

References

Bax, A. and Grzesiek, S. (1993) *Acc. Chem. Res.*, **26**, 131–138.

Clore, G.M. and Gronenborn, A.M. (1991) *Science*, **252**, 1390–1399.

Clubb, R.T. and Wagner, G. (1992) *J. Biomol. NMR*, **2**, 389–394.

Dötsch, V., Oswald, R.E. and Wagner, G. (1996a) *J. Magn. Reson.*, **B110**, 304–308.

Dötsch, V., Oswald, R.E. and Wagner, G. (1996b) *J. Magn. Reson.*, **B110**, 107–111.

Dötsch, V. and Wagner, G. (1996) *J. Magn. Reson.*, **B111**, 310–313.

Farmer II, B.T. and Venters, R.A. (1996) *J. Biomol. NMR*, **7**, 59–71.

Feng, W., Rios, C.B. and Montelione, G.T. (1996) *J. Biomol. NMR*, **8**, 98–104.

Friedrichs, M.S., Mueller, L. and Wittekind, M. (1994) *J. Biomol. NMR*, **4**, 703–726.

Gehring, K. and Guittet, E. (1995) *J. Magn. Reson.*, **B109**, 206–208.

Grzesiek, S. and Bax, A. (1992a) *J. Magn. Reson.*, **99**, 201–207.

Grzesiek, S. and Bax, A. (1992b) *J. Am. Chem. Soc.*, **114**, 6291–6293.

Grzesiek, S., Anglister, J. and Bax, A. (1993) *J. Magn. Reson.*, **B101**, 114–119.

Grzesiek, S. and Bax, A. (1993) *J. Biomol. NMR*, **3**, 185–204.

Ikura, M., Kay, L.E. and Bax, A. (1990) *Biochemistry*, **29**, 4659–4667.

Kay, L.E., Wittekind, M., McCoy, M., Friedrichs, M.S. and Mueller, L. (1992a) *J. Magn. Reson.*, **98**, 443–450.

Kay, L.E., Keifer, P. and Saarinen, T. (1992b) *J. Am. Chem. Soc.*, **114**, 10663–10665.

Lyons, B.A. and Montelione, G.T. (1993) *J. Magn. Reson.*, **B101**, 206–209.

Marion, D., Ikura, M., Tschudin, R. and Bax, A. (1989) *J. Magn. Reson.*, **85**, 393–399.

McCoy, M.A. and Mueller, L. (1992) *J. Am. Chem. Soc.*, **114**, 2108–2112.

Meadows, R.P., Olejniczak, E.T. and Fesik, S.W. (1994) *J. Biomol. NMR*, **4**, 79–96.

Montelione, G.T. and Wagner, G. (1989) *J. Am. Chem. Soc.*, **111**, 5474–5475.

Montelione, G.T. and Wagner, G. (1990) *J. Magn. Reson.*, **87**, 183–188.

Montelione, G.T., Lyons, B.A., Emerson, S.D. and Tashiro, M. (1992) *J. Am. Chem. Soc.*, **114**, 10974–10975.

Morris, G.A. and Freeman, R. (1979) *J. Am. Chem. Soc.*, **101**, 760–761.

Muhandiram, D.R. and Kay, L.E. (1994) *J. Magn. Reson.*, **B103**, 203–216.

Olejniczak, E.T., Xu, R.X., Petros, A.M. and Fesik, S.W. (1992) *J. Magn. Reson.*, **100**, 444–450.

Olejniczak, E.T. and Fesik, S.W. (1994) *J. Am. Chem. Soc.*, **116**, 2215–2216.

Palmer III, A.G., Fairbrother, W.J., Cavanagh, J., Wright, P. and Rance, M. (1992) *J. Biomol. NMR*, **2**, 103–108.

Powers, R., Gronenborn, A.M., Clore, G.M. and Bax, A. (1991) *J. Magn. Reson.*, **94**, 209–213.

Santoro, J. and King, G.C. (1992) *J. Magn. Reson.*, **97**, 202–207.

Shaka, A.J., Barker, P.B. and Freeman, R. (1985) *J. Magn. Reson.*, **77**, 274–293.

Tashiro, M., Rios, C.B. and Montelione, G.T. (1995) *J. Biomol. NMR*, **6**, 211–216.

Vuister, G.W. and Bax, A. (1992) *J. Magn. Reson.*, **98**, 428–435.

Wishart, D.S., Bigam, C.G., Holm, A., Hodges, R.S. and Sykes, B.D. (1995) *J. Biomol. NMR*, **5**, 67–81.

Wittekind, M., Metzler, W.J. and Mueller, L. (1993) *J. Magn. Reson.*, **B101**, 214–217.

Wüthrich, K. (1986) *NMR of Proteins and Nucleic Acids*, Wiley, New York, NY, U.S.A.

Yamazaki, T., Forman-Kay, J.D. and Kay, L.E. (1993) *J. Am. Chem. Soc.*, **115**, 11054–11055.

Yamazaki, T., Pascal, S.M., Singer, A.U., Forman-Kay, J.D. and Kay, L.E. (1995) *J. Am. Chem. Soc.*, **117**, 3556–3564.

Zimmerman, D.E., Kulikowski, C., Wang, L., Lyons, B. and Montelione, G.T. (1994) *J. Biomol. NMR*, **4**, 241–256.

Zimmerman, D.E. and Montelione, G.T. (1995) *Curr. Opin. Struct. Biol.*, **5**, 664–673.